Adaptive Voltage Stability Recovery in PV-Battery-based Power System under Dynamic Load Variations

S.D. Lumina*[1], M.E.S. Mnguni[2], N. Tshemese-Mvandaba[3]
Department of Electrical, Electronics and Computer Engineering, Faculty of Engineering and Built Environment, Cape Peninsula University of Technology, South Africa
*corresponding author's email: luminas@cput.ac.za

Abstract – *The rapid integration of renewable energy resources introduces significant unpredictability and uncertainty into modern power systems, raising concerns about voltage stability and grid optimization. This paper presents a real-time model and investigation of integrating a hybrid Photovoltaic (PV) and Battery Energy Storage System (BESS) into the IEEE-9 bus system under dynamic load conditions. A decentralized, adaptive PID-based droop voltage control mechanism is proposed to regulate the photovoltaic plant's output power via maximum power point tracking, while leveraging the BESS's fast dynamic response to smooth PV voltage deviations by injecting real and reactive power for rapid voltage recovery. A voltage-following control strategy is established to enable the hybrid system to stabilize bus voltages following sequential load variations. Using the Real-Time Digital Simulator (RTDS), grid-following operation is achieved, improving transient voltage recovery and reducing oscillations, outperforming PV-only integration.*

Keywords: *Battery energy storage system (BESS), grid following (GFL), photovoltaic (PV) integration, real-time digital simulator (RTDS), voltage stability.*

Article History
Received 26 January 2026
Received in revised form 25 February 2026
Accepted 28 March 2026

I. Introduction

Moving towards clean energy has accelerated the incorporation of renewable energy sources into the electric power system, with solar photovoltaics among the fastest-growing technologies. However, PV power is weather-dependent, intermittent, and grid-challenging, which, in some cases, limits its ability to provide adequate voltage stability in an unstable grid. Under regular grid operation, a synchronous generator constantly provides inertia and reactive power to maintain grid stability. Unfortunately, if dynamic load consumption continues to increase, the synchronous machine may exceed its capacity, posing a significant challenge to maintaining grid stability. In this context, PV integration is one of the solutions to provide grid power relief under dynamic load conditions. Alongside PV, the addition of BESS technology has attracted considerable attention as a complementary approach to enhance grid optimisation in a grid-following setup, where renewable energy is seen as contributing to grid stability. Unlike PV, the battery energy storage system can inject or absorb both real and reactive power, offering fast dynamic support during transient conditions [1]. Its ability to respond quickly may help smooth PV output fluctuations and mitigate voltage stability issues in the power system, especially given the impact of increased load consumption in a grid environment where synchronous machines face a reactive power shortage. In this regard, PV and BESS offer a promising approach to sustain voltage recovery and enhance transient stability. [2] Voltage stability is a crucial aspect of power system performance, describing the ability of an electrical system to maintain consistent voltage profiles at all system buses despite disturbances from a predetermined initial condition. Using the Continuous Power Flow (CPF) algorithm, the authors examine how voltage instability arises in the IEEE-9 bus system when the reactive power demanded by loads exceeds the system's capacity to supply it, leading to a progressive decline in voltage and eventual collapse. As load levels increase, both active and reactive power flows rise, causing generator excitation systems and voltage regulators to reach their operational limits. The CPF method repeatedly computes load flow solutions for different operating conditions using a predictor–corrector approach. It determines the stable-state voltage stability limit, represented by the 'nose point' of the P–V curve, which indicates the maximum transferable power. Starting from a base load, a tangent predictor estimates the next solution, and the Newton–Raphson corrector refines it. This iterative process

continues with gradual load increases until the system reaches the critical (voltage collapse) point. The CPF provides a reference value to position the maximum loading condition of the IEEE-9 bus, which is crucial in preventing total grid collapse. [3] Considering the basic concepts of power system resilience and vulnerability, the authors describe how power systems should be designed to enhance resilience and reduce vulnerability when faults occur during regular operation. They explain that the resilience of the power system refers to its capacity to withstand various disturbances and restore stable operating conditions after they are resolved[4]. Conversely, vulnerability in terms of power system stability refers to assessing the risks—such as economic losses and physical damage—that can arise from the system's ability to withstand unpredictable and undesirable events [5]. Two case studies using the IEEE-33 bus system were conducted to explore the importance of these concepts on voltage stability in power systems. In the first case, no distributed generation was considered, whereas in the second, its integration was effective. In both cases, the results indicated the need to incorporate robust requirements for power system resilience and vulnerability management into routine operations. The authors consider the electrical grid as one of the most essential infrastructures in power systems, and its security is vital for the proper dispatching of electricity to consumers. However, the functions of the electric power system must meet specific requirements regarding resilience and vulnerability. These requirements extend beyond protective devices to include the integration of distributed resources that enhance the power system's productivity and reliability.

Renewable energy systems (RES) neither provide the grid with inertia nor possess primary frequency control capabilities [6]. The integration of RES can reduce the spinning reserve and inertia of the power system. Introducing BESS into the grid-tied microgrid will not only improve system stability but also offer primary response capability due to increased frequency stability. BESS does not contribute to system inertia; its introduction in the grid is unlikely to cause further system instability. Subsequently, the increase in BESS capacity is likely to positively affect the angle speed and voltage response of the electrical power system. Thus. BESS has the potential to improve the system's steady-state frequency and voltages. Allocating batteries near loads helps distribute their power according to their control, although a negligible effect may arise due to generation or load response. But a BESS placed close to a microgrid, or synchronous generator, is unlikely to provide optimal response due to the grid power flow controller, unless a decentralised control mechanism is implemented to optimise the battery energy storage system's efficiency, especially in hybrid power systems. The Rafha grid case study was simulated using the Power System Simulator for Engineering (PSS/E).

As more concerns are raised about grid instability caused by various reasons, not limited to the depletion of fossil sources, wind power combined with solar power and battery storage facilities [7] can considerably reduce the impact on the power system caused by unstable energy supplies [8]. However, solar and wind energy are highly variable, so it is necessary to add a BESS to enhance the power quality of the electrical power system, leveraging their ability to utilise excess energy generated by wind and solar plants. The management of such mixed energy sources can only be achieved by considerable system optimisation. The proposed optimisation mechanism utilises integrated battery storage that operates in stages following the load of various patents. The authors presented a highly competitive algorithm, the Grey Wolf Optimiser, that delivers a joint optimal distribution of Renewable Distributed Generation (RDG) and system storage units to acquire economic profits and system stability. The method supervises the input power and the load demand to determine which power source, between wind, solar, and battery, must be utilised first. This mechanism allows excess power from renewable energy sources to be stored in the battery for subsequent use when the microgrid cannot provide sufficient power to maintain grid stability. By doing so, the authors have achieved significant progress in optimising the integration of power systems with multilevel energy sources to fully meet load demand and efficiently reduce curtailment of wind and solar power caused by uncertain conditions or poor power generation due to synchronous generator incapacity.

Investigate the feasibility of a control algorithm for the bidirectional interlinking converter (IC) to enable decentralised regulation and improve microgrid optimisation [9]. The proposed control enables coordinated sharing of power from renewable energy and battery systems to supply the power system with active and reactive power as required. The philosophy beyond the mechanism is for the various power plants to operate independently, without prior coordination, to respond to the control signal and act as a single compensator or to combine into a single entity. The IC algorithm also acts as an active power filter, restoring the microgrid's stability per IEEE-519 by granting reactive power and lowering harmonic levels beyond the 5% threshold. Thus, various causes of voltage instability, such as low power factor, voltage unbalance due to multiple factors beyond load consumption, harmonics, etc., can be mitigated by surplus power injection from a hybrid microgrid or a battery energy storage unit with the help of the IC algorithm.

Introduce wind-PV-battery-based hybrids for voltage reliability in a hybrid grid-tied environment. The variable nature of wind and solar power around the clock makes it challenging to provide stable, clean energy in either stand-alone or grid-tied mode [10]. One solution to the intermittent properties of renewable energy is to add battery storage to provide excellent frequency and voltage regulation when wind or solar generation is negatively

affected by weather conditions. The issue of a hybrid power plant isn't just about adding a battery to an already troubled system because of the unregulated microgrid[11]. Thus, a better design and adequate measures are discussed to establish a proper mechanism that ensures grid safety by implementing a power management system to handle power sharing between the microgrid and a control technique to regulate the state of charge (SOC) to ensure BESS productivity performance. A comprehensive control and power management system (CAPMS) is proposed to successfully regulate the direct and alternating current bus voltages and the constant frequency. The control strategy automatically controls each power plant's flexibility. It regulates power flow into the electric grid, regardless of operating conditions or disturbances caused by climate change, system faults, and load changes.

Previously conducted studies in the field of hybrid PV-BEES integration focused either on the energy management system level or on steady-state performance indices related to the battery's state of charge. Previous work in the same fields has shown less focus on the BESS's ability to mitigate bus voltage in benchmark transmission networks, such as the IEEE-9 bus system operating at 50Hz. Moreover, while PV inverters are often configured for maximum power point tracking (MPPT) and primarily deliver active power, the role of BESS in delivering fast-acting real and reactive power support during disturbances has not been thoroughly explored in this context. Few studies combine time-series (stochastic) load and PV variability with Continuous power flow, and coordination of inverter-based resources with a centralised control mechanism that does not consider each DER's capability limit in real time.

To address gaps in the study of hybrid PV-BESS, this paper examines the integration of hybrid PV-BESS into the IEEE-9 bus power system operating at 50Hz, focusing on the stability of grid-voltage-following control loops under load disturbances in real-time digital simulation. Introducing a novelty that focuses on the design of the adaptive GFL controller, whose Phase Loop Lock (PLL) adapts its response ability in real-time to load ramps and the photovoltaic intermittent nature. The BESS acts not just as a separate resource but rather as a potential active voltage stabiliser for the adaptive GFL PV inverter. Thus, novelty shifts from considering only PV as a probable GFL, while the BESS is seen as a peak shaving component. The RTDS simulation environment shows rapid control interactions that are often overlooked in offline software. The use of RTDS to tackle the issue of voltage stability in a grid following environment allows for providing strong results showing evidence of stability boundaries and grid performance capabilities while emulating events that may not be safe to simulate in a real power system. RTDS's ability allow to replicate real scenario in a safe environment.

Thus, the proposed control scheme regulates the PV to prioritise both active and reactive power generation through robust MPTT. At the same time, the BESS smart inverter is configured to provide fast voltage regulation by coordinating real and reactive power injection. The real-time simulation indicates that the hybrid PV-BESS system effectively enhances transient voltage recovery, reduces oscillatory responses, and improves overall system stability compared to PV-only configurations. The integration of the BESS considerably eases the burden on traditional generators by reducing the reliance of loads on a generator's power output. These results emphasise the crucial role of BESS in ensuring secure and reliable operation in renewable-rich power systems when a decentralised control algorithm is established to regulate each DER performance. The paper comprises several key sections. In Section 2, the proposed system is modelled. Moving to Section 3, different case studies based on IEEE-9 bus systems are presented to evaluate performance in RTDS. The focus shifts to power flow analysis during stable grid operation, with a specific simulation case illustrating the impact of expanded load consumption on voltage stability. The section also investigates the control mechanism for maintaining voltage stability, accounting for loading conditions and the feasibility of the proposed adaptive PID-droop voltage control. In Section 3, the paper presents results and discusses the success of the proposed control method, culminating in overall conclusions in Section 4.

II. System Modeling

Renewable energy plays a vital role in voltage regulation when it is integrated into the grid. Given their intermittent, weather-dependent nature, renewable energy sources such as PV may need to be combined with a battery energy storage system (BESS) to improve performance and optimise grid performance, especially when load conditions are considered.[12]. BESS state of charge in a Hybrid renewable environment is generally determined by the energy balance of solar systems and the load consumption. Fig. 1 shows the proposed schematic of integrating PV and BESS into the power system.

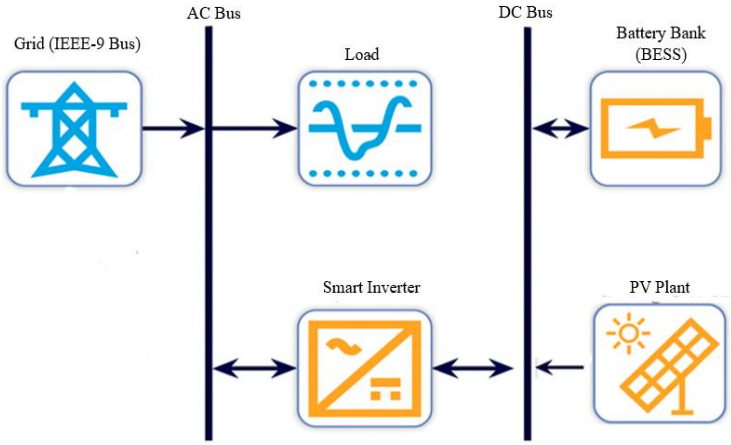

Fig. 1. Schematic of PV-BESS hybrid power system.

The PV is integrated into the grid to enhance voltage magnitude following changes in load conditions. At the same time, the BESS system is configured to simultaneously support the grid with sufficient power and absorb PV power when available. The configuration is preferred to enhance the grid-following capability for controlling grid voltage. Thus, leaving the grid in control of voltage regulation, while the BESS inverter injects small active power to support the grid even under any fault condition [13]. The power system under consideration is a reworked IEEE-9-bus system described in Fig. 2.

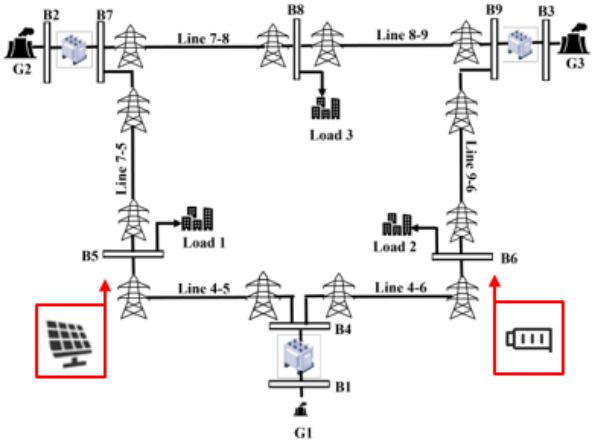

Fig. 2. Modified IEEE-9 bus system with PV-BESS systems[14].

The power system serves as a benchmark for voltage analysis, facilitates the implementation of various scenarios due to its generator configuration, and is complex enough to produce results that are close to those of a real-time system. It has been modified to suit the Southern African electrical pool with a frequency set at 50Hz. The system has three generators with capacities of 163, 72, and 85 megawatts (MW), and nine buses and transmission lines. Load conditions are observed at buses 5, 6, and 8 for voltage regulation purposes. System raw data are used in this paper's investigation.

A. Modelling of PV System

A photovoltaic system converts sunlight into electrical energy. A typical PV power system consists of interconnected PV cells, which are connected in parallel, in series, or in both configurations. The PV's inner configuration can be either a single diode or a double diode, depending on the model[15]. The PV model under consideration is a pre-built single-diode PV model in the RTDS library. The corresponding circuit for the single-diode configuration is indicated in Fig. 3.

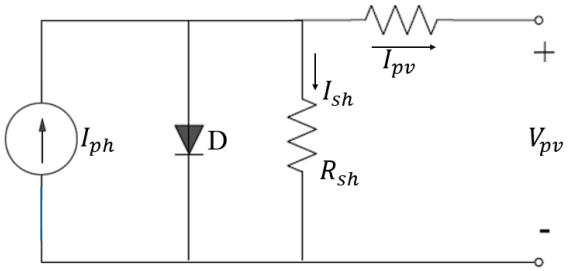

Fig. 3. PV cell single electrical equivalent circuit [16].

The figure above represents the electrical behaviour of a single diode PV module used for simulation purposes in RTDS. The following mathematical expressions in (1) and (2) are used to compute the I−V characteristics curve and the P−V curve for maximum power

$$I = I_{pv} - I_{sh}\left[\exp\left(\frac{V+IR_s}{nV_{pv}}\right) - 1\right] - \frac{V+IR_s}{R_{sh}} \quad (1)$$

And the thermal voltage of the cell can be expressed as:

$$V_{pv} = \frac{kT}{q} \quad (2)$$

Where I_{pv} describes the photocurrent, I_{sh} Is the expression of the diode saturation current,R_s the series resistance of the single diode PV model,R_{sh} describes the shunt resistance, n Is the diode's ideality factor typically 1 to 2. V_{pv} Is the thermal voltage of the cell and T Represent the cell temperature, q the electron charge and k the Boltzmann constant. The simple current equation required an iterative numerical solution to compute the PV's current output. The I-V characteristics curve of the PV can then be obtained at standard test conditions (STC) following the 3 key operating points of the PV module. These operating points are the short-circuit state, the open-circuit state, and the MPPT operating conditions, which are applied in the current research. Fig. 4 is a representation of a typical I-V curve of a Photovoltaic cell at STC.

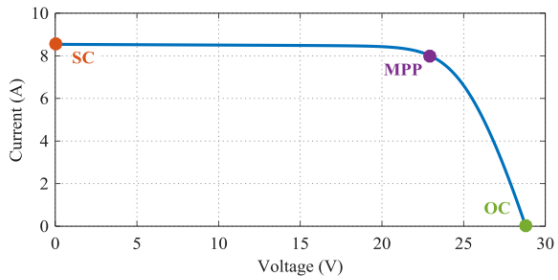

Fig. 4. Photovoltaic I-V curve at STC [16].

During the SC operating state, the PV current usually flows through both resistances since the diode does not conduct at that point. These conditions implied the circuit in a standard current divider, yielding in (3):

$$I_{sc} = \frac{I_{ph}R_{sc}}{(R_s+R_{sh})} \quad (3)$$

When considering the open condition OC, the PV circuit does not record any voltage drop along the series resistance. Thus, leaving the photocurrent to flow through the diode. If we consider equation 1, where zero current is applied, and two resistances are neglected, we get the open voltage as in (4):

$$V_{oc} = a.\ln\left(\frac{I_{ph}}{I_s}\right) \quad (4)$$

From which, the current in (5)

$$I_{ph} = I_s e^{V_{oc}/a} \quad (5)$$

The related equation to the calculation of the MPPT at standard conditions can also be deduced from the five parameters of the PV model as in (6) and (7):

$$V_{mpp} = V_{oc}\left(1 - \frac{1}{n\ln\left(\frac{I_{pv}}{I_{sh}}\right)}\right) \quad (6)$$

$$I_{mpp} = I_{sc}\left(1 - \frac{V_{mpp}}{V_{oc}}\right) \quad (7)$$

B. Battery Energy System Storage Modelling

Perfect battery sizing depends on various factors, including temperature correction, rated battery life, capacity, and maximum depth of discharge. [17]. The following equation (8) is used to estimate the battery capacity in ampere per hour.

$$B_{rc} = \frac{E_c D_s}{DOD_{max}\eta_t} \quad (8)$$

Where E_c Is the expression of the load articulated in ampere per hour (Ah), D_s Describe the battery's number of self-sufficiency periods, DOD_{max} Is the optimal state of the battery depth of discharge, considering a deep cycle battery, the rate for optimal DOD is 80%, η_t Defined the temperature correction factor. An integrated BESS into the grid is needed to recharge when PV output exceeds load demand automatically. The equation of the rate of charge of the BESS at time t Is calculated using the expression as in (9):

$$E_B(t) = E_B(t-1)(1-\sigma) + \left(\frac{E_{GA}(t)-E_L(t)}{\eta_{inv}}\right)\eta_{bat} \quad (9)$$

where $E_B(t)$ and $E_B(t-1)$ Describe the charge quantities of the BESS at t time and $(t-1)$, $E_{GA}(t)$ Does the renewable energy source generate the total energy, considering the losses in the controller, $E_L(t)$ Is the consumption of the load at the time t, η_{inv} and η_{bat} Are the efficiency of the smart-inverter and the charge effectiveness of BESS, s Is the amount of self-discharge correlated to the stored charge and the condition of battery strength. The charge capacity of the battery is subject to the limitations as indicated in (10):

$$E_{B_{min}} \leq E_B(t) \leq E_{B_{max}} \quad (10)$$

where $E_{B_{min}}$ and $E_{B_{max}}$ Are the minimum and maximum charge rates of the BESS.

When integrating BESS into grid-connected systems, the battery lifespan, depth of discharge, maintenance requirements, floating charge voltage, and State of Charge (SOC) are essential characteristics for optimising the hybrid renewable energy system. The BESS manufacturer provides some of these characteristics in the BESS datasheet; the unknown values can be computed using the equation provided. The SOC of the battery bank at the

time (t) can be determined by the given (11) below:

$$\mathrm{SOC(t)} = \mathrm{SOC\ (t-1)}.\left(1-\frac{\sigma.\Delta t}{24}\right)+ \frac{I_{bat}(t-1).\Delta t.\eta_{bat}}{C'_{bat}} \quad (11)$$

Where C'_{bat} Is the expression of the battery's normal capacity, Ah and η_{bat} Is the battery energy storage system's charging and discharging efficiency (generally, the round-trip efficiency).

C. Proposed Decentralized Control Mechanism

In the proposed control structure, two control mechanisms are proposed to enhance voltage stability in the power system following a change in load conditions. The first control algorithm, an adaptive PID droop loop voltage controller, is implemented via the PV voltage-source converter to regulate PV output power and mitigate voltage collapse. This controller combines a traditional PID controller for fast response with an adaptive droop voltage controller to push the PV to follow the grid voltage. Thus, leaving the grid with the sole ability to control the voltage. The PV plant is set to supply a portion of the power required during load conditions, using maximum power point tracking to maintain optimal generation throughout the control process.[18]. The mathematical formulation of the adaptive PID droop control scheme is expressed as:

$$Q_{ref} = \left(K_{q0} + \alpha\left|V_{ref} - V_{grid}\right|\right)\left(V_{ref} - V_{grid}\right) + K_p e(t) + K_i \int e(t)dt + K_d \frac{de(t)}{dt} \quad (12)$$

$$P_{ref} = P_{MPPT} - K_{pv}(t)\left(V_{ref} - V_{grid}\right) \quad (13)$$

Where $e(t) = V_{ref} - V_{grid}$, this represents the voltage deviation at PCC,K_{q0} the nominal droop gain to turn the controller, α represents the adaptive gain coefficient to track the load ramping, and K_i,K_d and $K_p e$ are respectively the integral, derivative gains, and the proportional of the PID mechanism coupled with K_{q0} and $K_{pv}(t)$ are the adaptive gains to create a voltage-dependent power injection from the PV. Therefore, allowing the PV to primarily support the voltage using reactive power and active power during voltage stress. Thus, leaving the grid to dominate the voltage control as per grid following concept.

The second control mechanism is a PID controller for BESS integration. The BESS is regulated to continuously provide extra power to the grid, thus focusing on the ancillary service during both regular operation and abnormal operation of the power system[19] . The BESS is connected to the IEEE-9 bus system via a bidirectional inverter, allowing it to discharge and charge while following the grid voltage. BESS can only charge when surplus PV power is available. The mathematical expression of the BESS control loop for continuous operation support condition with BESS injecting considerable power even under steady state operating condition, can be defined as:

$$P_{BESS} = P_{bias} + K_p\left(V_{ref} - V_{bus}\right) + K_i \int \binom{V_{ref} -}{V_{bus}} dt + K_d \frac{d(V_{ref} - V_{bus})}{dt} \quad (14)$$

$$Q_{BESS} = K_{pQ}\left(V_{ref} - V_{bus}\right) + K_{iQ} \int \left(V_{ref} - V_{bus}\right)dt + K_{dQ} \frac{d(V_{ref} - V_{bus})}{dt} \quad (15)$$

Where P_{bias} describes the continuous operation of BESS even when $\left(V_{ref} - V_{bus}\right) = 0$, $K_d \frac{d(V_{ref} - V_{bus})}{dt}$ is the derivative term for dampers' oscillations used to improve dynamic stability during load dynamics,$K_p\left(V_{ref} - V_{bus}\right)$ the proportional term that defines the immediate response of BESS to the voltage drop, and $K_i \int V_{ref} - V_{bus}$ shows the adaptive ability of the controller to keep following the voltage variation in the system. To add to the controller is Q_{BESS}, which describes the ability of the BESS to inject of absorbed the reactive power with K_{pQ} ,K_{iQ}, and K_{dQ} to be respectively the proportional gain, the internal gain and the derivative gain to determine the fast response of BESS reactive power to voltage deviation, and constant monitoring of voltage deviation. Overall, the BESS PID controller enhances the grid following capability by regulating both active and reactive power to support the hybrid power system. Fig. 4 shows the adaptive PID droop voltage controller implemented in RTDS to synchronise the PV with the power system, while Fig. 5 shows the PID controller for BESS integration into the same power system.

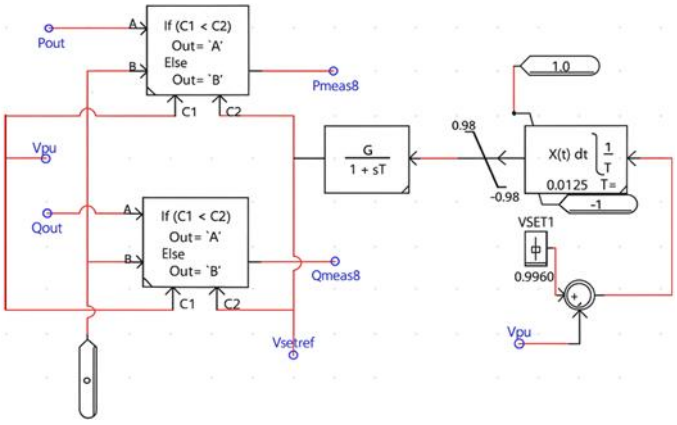

Fig. 5. RTDS adaptive PID-drop voltage controller for PV synchronization in the Grid Following loop.

Fig. 5 describes the structure of the voltage regulator for monitoring PV output power in a grid-following environment. The measured voltage at the point of common coupling, Vpu, and the converter output (Qout) and (Pout) are compared with reference values to issue an error using a conditional decision algorithm, which then issues a command. The outcome decision is then used to determine the required amount of the active (Pmeas8) and reactive power (Qmeas8) outputs to be sent to the grid-following Voltage Source converter. A filtered voltage reference is produced by a first-order dynamic block and an integrator driven by the voltage setpoint (VSET1), ensuring smooth voltage tracking during PV fluctuations.

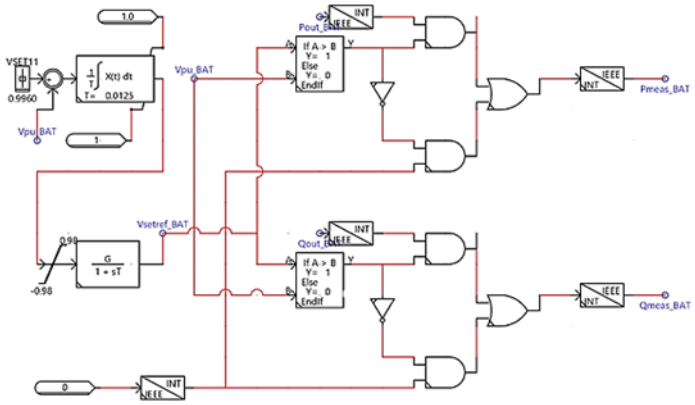

Fig. 6. RTDS PID Controller for BESS integration in Grid Following Power

Fig 6. describes the battery inverter control logic that compares the per unit voltage (Vpu_BAT) at the point of coupling and compares it to the voltage reference (Vsetref_BAT) to decide when the BESS should supply or absorb active and reactive power. The comparator block in the logic generates signals based on the voltage condition. The signal is passed through the gates AND/OR logic to stimulate the integrator blocks that produce Pmeas_BAT and Qmeas_BAT, the controller is built at the converter level to ensure that the battery injects power in small quantities for grid oscillation, to inject power when the voltage error is above the threshold reference, and at least to absorb or limit the power when the measured voltage falls below the prefixed threshold. Thus, the controller, via the bidirectional converter, allows coordination of both active power (P) and reactive power (Q) in a grid-following mode.

III. Simulation and Results

Three case studies were conducted to investigate the voltage profile under load conditions, followed by analysis under PV integration and, lastly, under both PV and BESS integration. All three cases were performed gradually to observe changes in the voltage pattern under various conditions, while considering the grid-following ability to control voltage under renewable energy penetration. For the load condition, the load consumption increased by 4% rise from the initial operation condition,

applied in steps of 2 seconds. Results of the voltage profile are depicted in Table I.

TABLE I
SYSTEM PERFORMANCE UNDER LOAD CONDITIONS

Bus No	Bus Type	Voltage (p.u.)	P_load (MW)	Q_load (MVar)	P_gen (MW)	Q_gen (MVar)
1	Slack	1.032	0.00	0.00	**128.6**	**102.20**
2	PV	0.988	0.00	0.00	**219.94**	**56.334**
3	PV	0.980	0.00	0.00	**141.97**	**20.198**
4	PQ	0.977	0.00	0.00	0.0	0.0
5	PQ	**0.916**	**200**	**84.7**	0.0	0.0
6	PQ	**0.932**	**144**	**49.6**	0.0	0.0
7	PQ	0.963	0.00	0.0	0.0	0.0
8	PQ	**0.936**	**160**	**57.9**	0.0	0.0
9	PQ	1.323	0.00	0.0	0.0	0.0

The results in Table I illustrate the system's performance under varying load conditions. The remarkable drop in voltage on buses 5, 6, and 8 is notable, as the traditional generator's power output is increasing to meet the growing demand. The results can also be illustrated in Fig. 7(a),7(b) and 7 (c), showing the voltage drops below the permissible level for voltage stability.

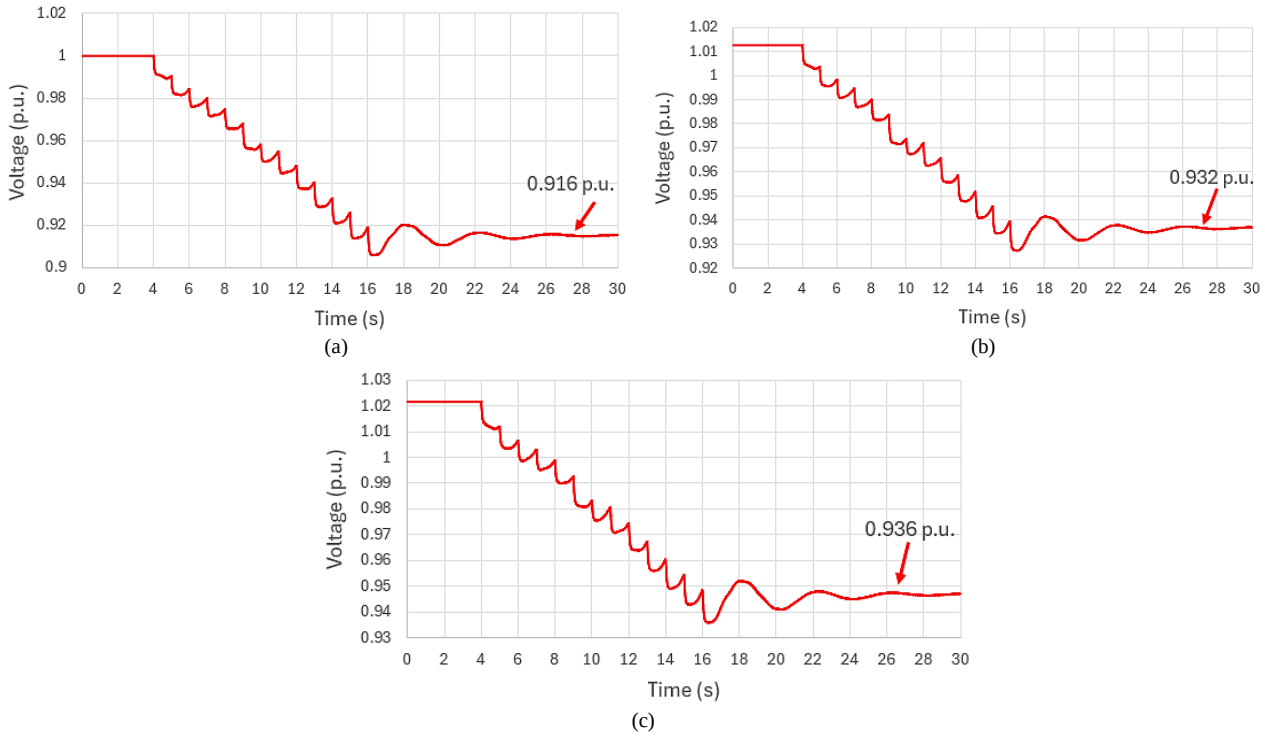

Fig. 7. Load increase impact on voltage at various buses. (a) variation at bus 5. (b) Voltage drops at bus 6. (c) Bus 8 Voltage under load Conditions

Considering that the generator governors failed to recover the voltage from the impact of the load condition on the 16th second, a second case study is therefore undertaken with the integration of a PV power plant at Bus 5 of the IEEE-9 bus system. The PV is synchronized via a voltage-source converter with an LCL filter capacitor to suppress high-frequency switching harmonics. Results of the case are shown in Table II and Fig.8(a)-Fig.8(c).

TABLE II
SYSTEM PERFORMANCE UNDER PV INTEGRATED THROUGH PID-DROOP CONTROLLER

Bus No	Bus Type	Voltage (p.u.)	P_gen (MW)	Q_gen (MVar)

1	Slack	1.0342	**133.6**	**74.405**
2	PV	0.9909	**229.1**	**37.012**
3	PV	0.9816	**143.02**	**9.673**
4	PQ	0.9955	0.0	0.0
5	PQ	**0.9636**	0.0	0.0
6	PQ	**0.9748**	0.0	0.0
7	PQ	0.9509	0.0	0.0
8	PQ	**0.9737**	0.0	0.0
9	PQ	1.0323	0.0	0.0

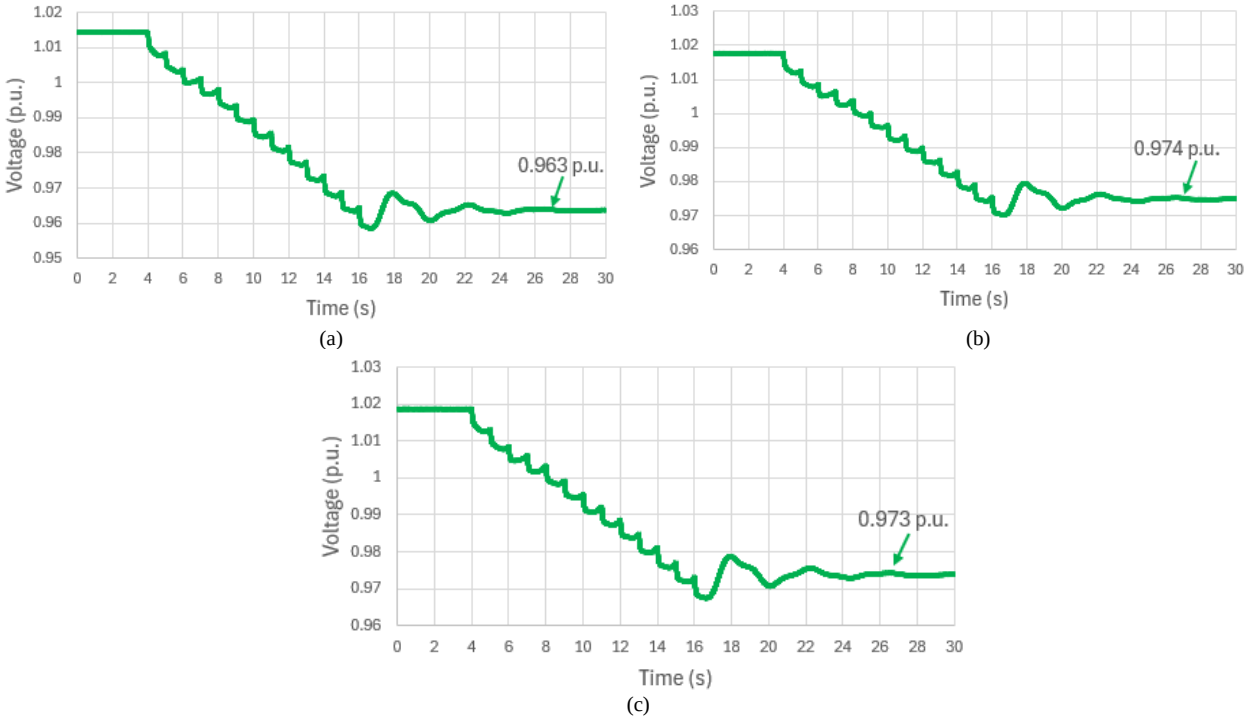

Fig. 8. Variation of voltage profile under PV penetration. (a) Bus 5 voltage improved. (b) Bus 6 voltage recovery and (C) bus 8 voltage improved under PV penetration

The results in Table II illustrate the system's behaviours under increasing load conditions. A noticeable voltage recovery occurs at buses 5, 6, and 8 due to the PV output power's impact on the adaptive PID droop controller. These values indicate that the controller partially recovered the grid's voltage magnitude. Thus, allowing the grid the ability to control the voltage regulation response. Fig. 8(a).8(b), and 8(c) confirm the controller's ability, with improved voltage at buses 5, 6, and 8.

To further enhance voltage stability, a BESS is integrated for further investigation, considering load conditions and PV impacts. The BESS is incorporated at bus 6 of the power system, close to the slack bus and the PV plant, for quick response to system changes. The BESS, through its bidirectional converter, can enable rapid response by injecting both active and reactive power into the IEEE-9 bus system. It is also designed to charge solely from surplus PV power. This approach is expected to increase the power system's renewable energy hosting capacity and reduce reliance on slower generators' control mechanisms.[20][21]. Simulation results related to the impact of BESS integrated into an existing PV power system, considering load conditions, are duplicated in Table III and further displayed in Fig.9 (a-b) to Fig.11 (a-b).

TABLE III
OVERALL SYSTEM PERFORMANCE CONSIDERING ALL CASES SIMULATED IN RTDS

Bus No	Voltage p.u. (Base)	Voltage Under load Conditions	Voltage Under PV Penetration	Voltage Under PV-BESS Penetration	P_gen Under load conditions (MW)	P_gen After PV-BESS Penetration (MW)	Q_gen Under Load Conditions (MVar)	Q_gen After PV-BESS Penetration (MVar)
1	Slack	1.032	1.037	1.037	**128.6**	**71.45**	**102.20**	**54.18**

2	PV	0.988	0.997	0.995	**219.94**	**232.4**	**56.334**	**26.13**
3	PV	0.980	0.998	0.998	**141.97**	**129.6**	**20.198**	**0.243**
4	PQ	0.977	1.004	1.004	0.0	0.0	0.0	0.0
5	PQ	**0.916**	**0.963**	**0.967**	0.0	0.0	0.0	0.0
6	PQ	**0.921**	**0.974**	**0.988**	0.0	0.0	0.0	0.0
7	PQ	0.963	0.984	0.984	0.0	0.0	0.0	0.0
8	PQ	**0.936**	**0.973**	**0.968**	0.0	0.0	0.0	0.0
9	PQ	1.323	0.998	0.999	0.0	0.0	0.0	0.0

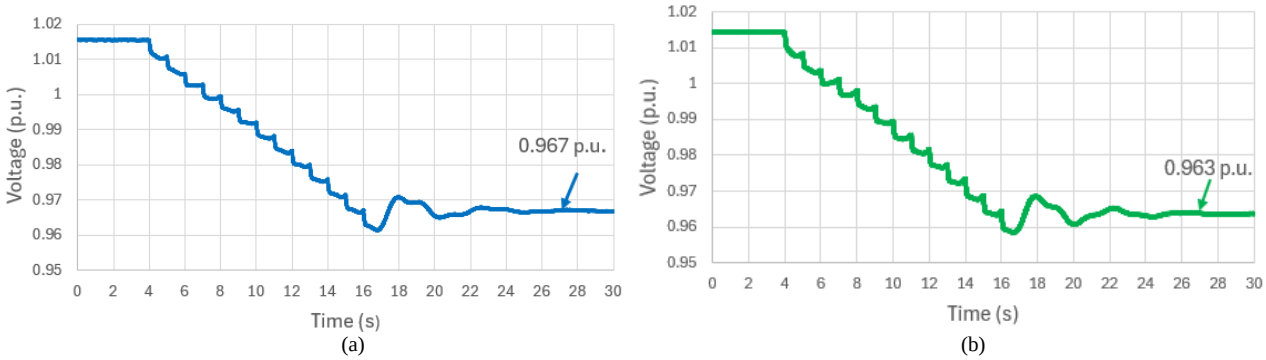

(a) (b)

Fig. 9 Comparison of bus 5 voltage improvement following PV only integration 9(a) vs Hybrid PV-BESS 9(b).

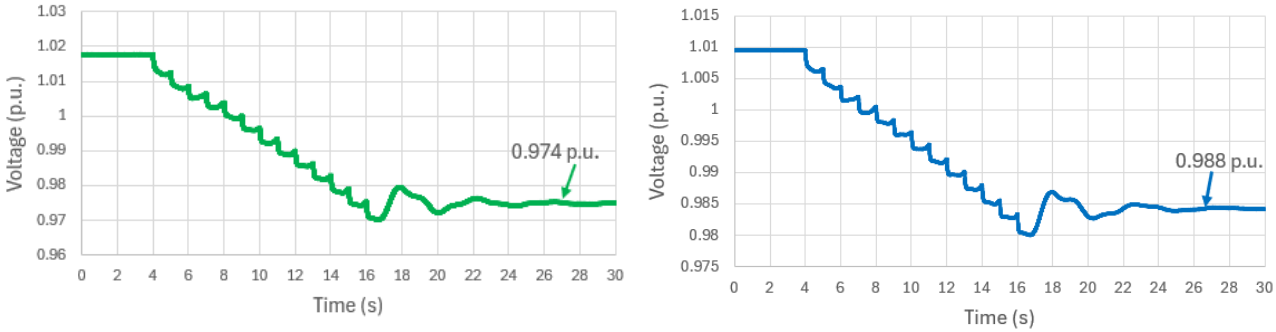

(a) (b)

Fig. 10. Comparison of the voltage profile under PV penetration only 10(a) vs. the voltage profile under PV- BESS integration 10 (b) at bus 6.

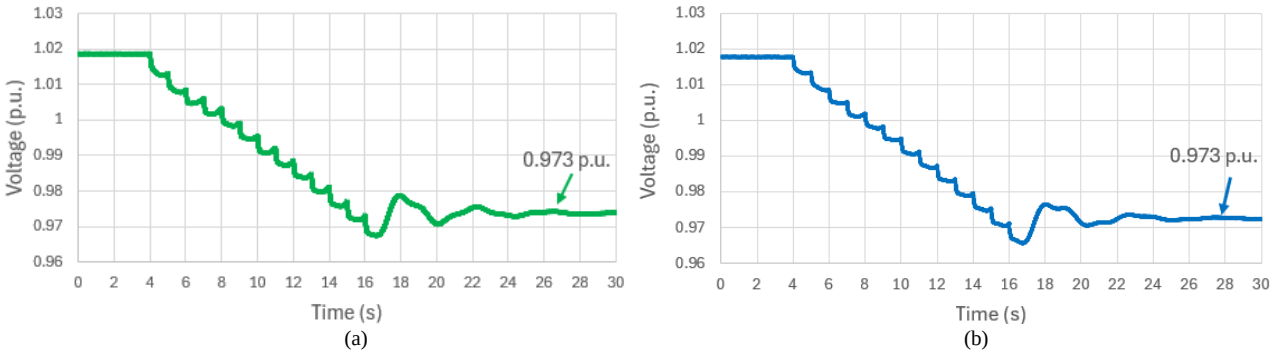

(a) (b)

Fig. 11. Comparison of the voltage profile under PV penetration only 10(a) vs. the voltage profile under PV- BESS integration 10 (b) at bus 8.

RTDS simulation results for the $50H_Z$ −IEEE-9 bus under load conditions and renewable energy integration shows that, compared to the PV-alone integration case, the BESS integration provides a clear, fast response with rapid reactive power support, thereby reducing fluctuations and shortening recovery time at all affected buses. In the figures above, the PV support itself restores the voltage magnitude after disturbance; however, with the integration of the BESS, the voltage recovery is achieved much faster, within 20 seconds after disturbance. This voltage enhancement is due to the BESS's fast control response to enable both active and reactive power exchange. Thus, as

shown in all figures, PV-BESS integration also mitigates post-disturbance voltage dips, improving dynamic voltage stability in the power system.[22] For Fig. 10, the BESS integration shows a strong influence when the voltage magnitude is reduced. This is due to the BESS's charging state when absorbing active power during a PV surplus. Thus, confirm the controller's ability to influence the PCC voltage through active and reactive power exchange while charging from PV power surplus. Typically, the presence of BESS reduces the voltage at bus 6 by absorbing active power while maintaining appropriate reactive power, enabling the BESS to support the PCC voltage in a weak power system.[23]. The BESS connected at Bus 6 has little influence on the voltage profile at Bus 8, as shown in Fig. 11. The BESS's impact diminishes with the power system configuration, placing Bus 8 far from the Battery. Further studies are required in this regard to identify an adequate solution, such as integrating additional renewable energy resources, such as wind power, and investigating mixed renewable energy integration. Table IV is a summary of the power generation of the IEEE-9 bus system during various test conditions at a frequency of $50Hz$ As applicable in the Southern Africa pool.

TABLE IV
POWER GENERATION VARIATION DURING VARIOUS CASES

Case Comparison	Generated (MW)	Generated (MVar)
Base case	319.826	22.879
Load Condition	**490.560**	**260.53**
PV-BESS Penetration	**433.201**	**80.510**

IV. Conclusion

The paper explores the integration of both PV and BESS in a weak IEEE-9 bus system, focusing on the implementation of a decentralized control algorithm based on an adaptive PID droop voltage control to enhance voltage stability at weak buses by providing a quick, controllable, and adequate response of both active and reactive power, especially during load conditions. Comparing the impact of PV-only with that of PV-BESS integration, the RDTS investigation shows that coordinated PV-BESS integration is an effective solution for mitigating voltage when proper decentralized control is in place. The PID controller's capability also highlights that it is possible to increase the renewable energy hosting capacity of a power system while maintaining the grid-following ability.

Conflict of Interest

The authors declare no conflict of interest in the publication process of the research article.

Author Contributions

Sampi D. Lumina: Conceptualization, Investigation, Data collection, analysis, writing–original draft preparation; M.E.S. Mnguni and N. Tshemese-Mvandaba: Supervision, draft review and editing. All authors have approved the final manuscript for publication in the journal.

References

[1] D. Sanin-villa and L. F. Grisales-noreña, "Coordinated Active – Reactive Power Scheduling of Battery Energy Storage in AC Microgrids for Reducing Energy Losses and Carbon Emissions," 2025.

[2] K. Anthony and V. Arunachalam, "e-Prime - Advances in Electrical Engineering, Electronics and Energy Voltage stability monitoring and improvement in a renewable energy dominated deregulated power system : A review," *e-Prime - Adv. Electr. Eng. Electron. Energy*, vol. 11, no. January 2024, p. 100893, 2025, doi: 10.1016/j.prime.2024.100893.

[3] U. Shahzad, "The concept of vulnerability and resilience in electric power systems ABSTRACT," *Aust. J. Electr. Electron. Eng.*, vol. 00, no. 00, pp. 1–8, 2021, doi: 10.1080/1448837X.2021.1943861.

[4] S. D. Lumina, M. E. S. Mnguni, and Y. D. Mfoumboulou, "Photovoltaic Controller Design Based on Adaptive Volt / Var Algorithm to Stand the Impact of Load Increase in Grid Tied Microgrid System," vol. 12, no. 3, 2023, doi: 10.18178/ijeetc.12.3.186-193.

[5] A. Lopez, H. Zargaryan, and M. Avendaño, "Climate Vulnerability Assessment in Power Systems," 2023, doi: 10.1109/PESGM52003.2023.10252207.

[6] A. S. Alsalman, T. Alharbi, and A. A. Mahfouz, "Enhancing the Stability of an Isolated Electric Grid by the Utilization of Energy Storage Systems: A Case Study on the Rafha Grid," *Sustain.*, vol. 15, no. 17, 2023, doi: 10.3390/su151713269.

[7] Z. Wang *et al.*, "Study on the Optimal Configuration of a Wind-Solar-Battery-Fuel Cell System Based on a Regional Power Supply," *IEEE Access*, vol. 9, pp. 47056–47068, 2021, doi: 10.1109/ACCESS.2021.3064888.

[8] V. Application, "Hybrid Power Management Strategy with Fuel Cell , Battery," 2022.

[9] J. Jayaram, M. Srinivasan, N. Prabaharan, and T. Senjyu, "Design of Decentralized Hybrid Microgrid Integrating Multiple Renewable Energy Sources with Power Quality Improvement," *Sustain.*, vol. 14, no. 13, 2022, doi: 10.3390/su14137777.

[10] M. Patel and S. Bohra, "Power management of grid-connected PV wind hybrid system incorporated with energy storage system," *Futur. Energy*, vol. 2, no. 3, pp. 7–19, 2023, doi: 10.55670/fpll.fuen.2.3.2.

[11] S. D. Lumina, M. Elvis Mnguni, and N. Tshemese-Mvandaba, "Enhancing Grid Resilience Through Hybrid Renewable Energy Systems: Challenges, Control Strategies, and Future Directions: A Review," *Proc. 33rd South. African Univ. Power Eng. Conf. SAUPEC 2025*, pp. 1–6, 2025, doi: 10.1109/SAUPEC65723.2025.10944348.

[12] S. Pei, C. Han, P. Zhang, and J. Xu, "Energy Storage Configuration Considering Battery Characteristics for Photovoltaic Power Station," *2021 4th Int. Conf. Energy, Electr. Power Eng. CEEPE 2021*, pp. 120–124, 2021, doi: 10.1109/CEEPE51765.2021.9475796.

[13] T. Falope, L. Lao, D. Hanak, and D. Huo, "Hybrid energy system integration and management for solar energy: A review," *Energy Convers. Manag. X*, vol. 21, no. January, p. 100527, 2024, doi: 10.1016/j.ecmx.2024.100527.

[14] R. Vaish, "Challenges Posed by Renewable Energy Source Integration to Machine Learning based Power System Fault Diagnosis," *2024 IEEE Int. Commun. Energy Conf.*, pp. 1–5, doi: 10.1109/INTELEC60315.2024.10679013.

[15] S. D. Lumina, M. E. S. Mnguni, and Y. D. Mfoumboulou, "Stability Evaluation of Non-ideal Grid-tied Photovoltaic on IEEE-9 Bus System," vol. 6, no. 2, pp. 0–7, 2023.
[16] E. I. Batzelis, "Simple PV Performance Equations Theoretically Well-Founded on the Single-Diode Model," pp. 1–9, 2017.
[17] B. Bhandari, K. T. Lee, G. Y. Lee, Y. M. Cho, and S. H. Ahn, "Optimization of hybrid renewable energy power systems: A review," *Int. J. Precis. Eng. Manuf. - Green Technol.*, vol. 2, no. 1, pp. 99–112, 2015, doi: 10.1007/s40684-015-0013-z.
[18] M. Ullah, Y. Guan, M. A. Barrios, and J. C. Vasquez, "Dynamic Response of Droop-Controlled Grid-Forming Inverters Under Varying Grid Impedances for Enhanced Stability in Microgrids," pp. 1–22, 2025.
[19] F. C. Mushid, "Battery Energy Storage for Ancillary Services in Distribution Networks : Technologies, Applications, and Deployment Challenges — A Comprehensive Review," 2025.
[20] J. K. Bhutto *et al.*, "Coordinated Hybrid VAR Compensation Strategy with Grid-Forming BESS and Solar PV for Enhanced Stability in Inverter-Dominated Power Systems," pp. 1–24, 2025.
[21] N. Tshinavhe, M. Ratshitanga, and N. Tshemese-mvandaba, "Review of Adaptive Load Frequency Control Strategies for Improving Wind Power Plant Integration," *2024 32nd South. African Univ. Power Eng. Conf.*, pp. 1–6, doi: 10.1109/SAUPEC60914.2024.10445051.
[22] G. Macharia, L. Mogaka, and A. Wangai, "Enhancing grid stability and resilience through BESS optimal placement and sizing in VRES-dominated systems," *Energy Reports*, vol. 13, no. January, pp. 1764–1779, 2025, doi: 10.1016/j.egyr.2025.01.028.
[23] J. Petit-homme, "Battery Energy Storage System Allocation for Voltage Support and Congestion Mitigation".